RESEARCH ARTICLE

Geoarchaeology An International Journal    WILEY

# Micro-stromatolitic laminations and the origins of engraved, oxalate-rich accretions from Australian rock art shelters

Helen Green[1] | Andrew Gleadow[1] | Damien Finch[1] | Cecilia Myers[2] | Jenna McGovern[1]

[1]School of Geography, Earth and Atmospheric Earth Sciences, The University of Melbourne, Melbourne, Victoria, Australia

[2]Theda Station, Dunkeld Pastoral Co. Pty Ltd, Kununurra, Western Australia, Australia

**Correspondence**
Helen Green, School of Geography, Earth and Atmospheric Earth Sciences, University of Melbourne, Melbourne, VC 3010, Australia.
Email: Greenhe@unimelb.edu.au

Scientific editing by Sarah Sherwood.

## Abstract

Distinctive, dark-coloured, glaze-like mineral accretions are common on low-angle surfaces in sandstone rock shelters in the Kimberley region of north-western Australia, where they provide an attractive medium for the production of deep engravings, and occasionally, are associated with painted rock art. These accretions form within the shelter dripline and are similar to those reported from other sites around the world, where they have been used for radiocarbon dating of associated rock art. This study uses extensive field observations and mineralogical analysis of 77 such oxalate-rich accretions collected at 41 different sites across a wide area of the north Kimberley region. The mineralogy of these accretions is dominated by well-crystallised calcium oxalate and sulphate minerals, most commonly whewellite and gypsum, with significant occurrences of phosphates in some samples. The accretions are typically several millimetres thick and characterised by distinctive internal laminations that show regular stacked undulations, giving a stromatolitic appearance under the microscope. Together with other apparently microbial features observed under the scanning electron microscope, these features provide strong support for a microbiological origin for these oxalate-rich accretions. The well-crystallised nature of the oxalates and the preservation of fine laminar features within the accretions supports their use for radiocarbon dating.

### KEYWORDS
engravings, laminations, mineral accretions, oxalate, rock shelter, stromatolitic

## 1 | INTRODUCTION

Direct dating of charcoal (Quiles et al., 2016; Valladas et al., 2001) and other organic constituents (McDonald et al., 2014; Russ et al., 1990) in rock art paintings has been used to provide ages as close to the timing of the art as possible. However, in areas where ochre (iron oxide) is the preferred pigment choice, or art is engraved,

insufficient organic material can render direct dating particularly difficult and, in these regions, alternative dating methods and materials must be explored (e.g., Finch et al., 2020, 2021; Ross et al., 2016). Mineral accretions, displaying a clear relationship with pigment or engravings, offer a means of providing minimum and maximum age constraints for the associated art, should they be reliably dated. In limestone provinces, uranium-series dating methods

applied to calcium carbonate accretions have been used to provide bracketing ages for associated rock art (Aubert et al., 2007, 2014, 2018, 2019; Hoffmann et al., 2018; Pike et al., 2012), whilst radiocarbon dating of oxalate-rich accretions has been used to date motifs in geological environments where secondary calcium carbonates are absent (e.g., Jones et al., 2017; Smith et al., 2009; Watchman, 1993).

The Kimberley region in north-western Australia is host to one of the richest assemblages of rock art in the world, consisting predominantly of ochre paintings with some engravings and anthropomorphic markings in sandstone rock shelters across the region. The rock art in this region has been extensively recorded, resulting in the development of a detailed stylistic sequence broadly relating to six separate styles (e.g., Crawford, 1977; Donaldson, 2012; Lewis, 1997; Walsh, 1994, 2000; Welch et al., 1993, 2015), but until recently (Finch et al., 2020; 2021; Ross et al., 2016), challenges around both direct and indirect dating methods meant that very few motifs from the earlier art styles had absolute age constraints. Comparative to painted rock art, engraved art is particularly understudied in the Kimberley despite ground cupules being considered the oldest style in the sequence (Veth et al., 2017; Walsh, 2000). Importantly, engraved art is found almost exclusively etched into distinctive mineral accretions, often homogeneous in their dark brown-black colouration and smooth, glossy appearance. Previous work by the authors identified these deposits as one of four mineral accretion systems occurring in sandstone rock shelters in the Kimberley. Green et al. (2017a, 2017b) characterise the glaze deposits with a mineralogy rich in the monohydrated calcium oxalate whewellite ($CaC_2O_4 \cdot H_2O$) and less commonly, the dehydrated weddellite ($Ca(C_2O_4)_2(H_2O)$), as well as calcium sulphates gypsum ($CaSO_4 \cdot 2H_2O$) and anhydrite ($CaSO_4$).

The carbon component of the oxalate minerals, characteristic of this system, provides a clear opportunity for radiocarbon dating and has been used globally to date associated rock art (e.g., Jones et al., 2017; Ruiz et al., 2012; Watchman, 1993). In the Kimberley, laminated, oxalate-rich mineral accretions from rock shelters have been previously radiocarbon dated (Watchman et al., 2001, 2005), and their formation has been attributed to a microbiological mechanism, enabling a link to be made between the layering and environmental change. However, an improved understanding of how the appearance, occurrence and composition of these accretions vary temporally and spatially in the Kimberley is imperative to an improved understanding of their formation and, in turn, will facilitate an assessment of the reliability of such accretions as rock art dating tools and potential palaeoenvironmental archives for the region.

Here, detailed field observations are used alongside laboratory analyses of 77 accretion samples collected at 41 sites across northeast Kimberley (Figure 1) to identify key characteristic features both within and between accretion samples. A formation mechanism similar to that identified for oxalate-rich deposits in other regions (Roberts et al., 2015; Russ et al., 1996) and developed from that previously proposed for the Kimberley region (Watchman et al., 2001) is outlined and used to emphasise the requirement to

identify the oxalate-producing microbial communities before clear links to palaeoenvironmental conditions can be made.

## 1.1 | Setting

The landscape of the Kimberley region in north-western Australia is dominated by flat-lying, Paleoproterozoic sandstones and orthoquartzites of the Kimberley Basin, covering an area of ~135,000 km², with most rock art found in open rock shelters within the Warton and Wunaamin Miliwundi (formally King Leopold) sandstone formations (Figure 1). The monsoonal climate of the region is characterised by a wet season occurring between October and April, when rainfall is sourced primarily from the Indian Ocean to the north-west and represents ~90% of the annual total (Denniston et al., 2013), and a dry season between May and September, when air masses migrate from the continental interior to the south-east (HYSPLIT, 2020). Bushfires are common throughout the drier months (Northern Australian Fire Information [NAFI] Website, 2020), many of which are ignited naturally by lightning strikes. Vegetation across the region is chiefly open savannah woodland (Legge et al., 2016) and bunch grass, with major vegetation mosaics focussed in the central research area.

## 2 | MATERIALS AND METHODS

### 2.1 | Field sampling

Accretions were collected from sandstone rock shelters across the Drysdale, Barton and King George River catchments in north Kimberley (Figure 1) during the wet and dry seasons of 2014–2019. Key features of the accretions (colour, texture, thickness), their occurrence within the shelters and, where relevant, their spatial association with rock art were photographed and recorded directly using a custom application on iPads in the field. Samples were collected using a small cold-chisel and hammer directly onto a sheet of aluminium foil and targeted to minimise the impact on any art, whilst also removing intact pieces to preserve their internal structure. Target materials were taped to the surface before sampling to ensure that no pieces were lost and each sample collected from an archaeological site was removed in close collaboration and consultation and with explicit permission from a Traditional Owner from the Balanggarra native title region, present on site. A further 6 samples of shelter floor sediments were also collected to provide contextual information for the accretion materials. 75 samples were collected in shelters containing rock art and 2 samples were collected and many accretions were observed in shelters without rock art or other evidence of human activity. Specific locations of the rock shelters are not disclosed in this study to protect sites from unauthorised visitation and to respect the wishes of our indigenous partners. However, site localities are given a reference number that correlates to an access-controlled site catalogue stored on a secure, dedicated server held by project partners.
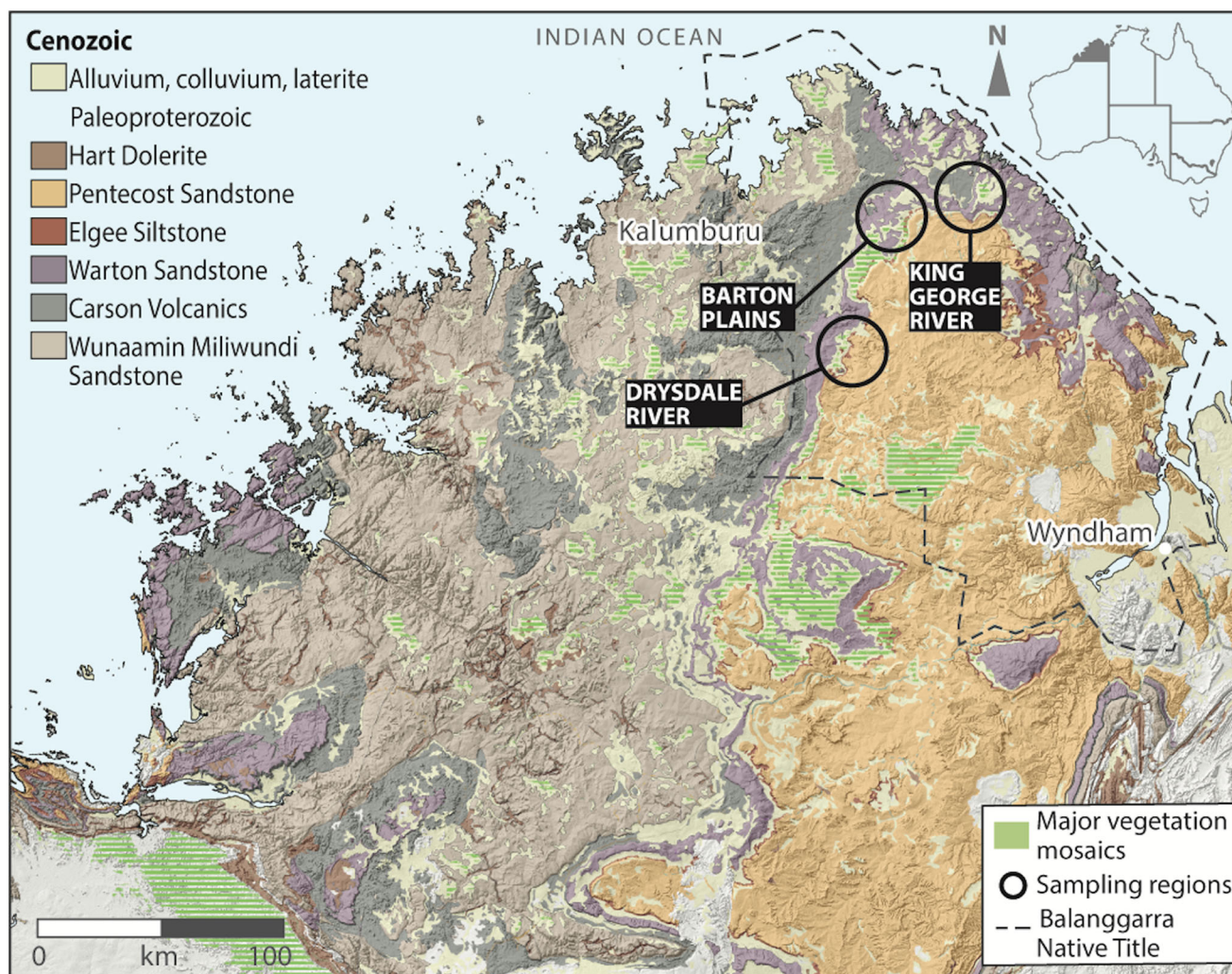
**FIGURE 1** Geological map displaying three main sampling regions located predominantly in the Warton Sandstone units. Illustration adapted from Green et al. (2017a) [Color figure can be viewed at wileyonlinelibrary.com]

## 2.2 | Internal composition

A range of analytical techniques were used to characterise the mineralogy of 77 samples and to understand the distribution and concentration of minerals within the accretion internal structures. Where sufficient material was available, samples were split in the laboratory, with one half analysed as loose fragments using scanning electron microscopy (SEM) and energy-dispersive X-ray spectrometry (EDS) to identify mineral distribution and morphology. This piece was then powdered for X-ray diffraction analysis (XRD), providing information on the bulk mineralogical composition of the accretions. The other sample half was mounted in epoxy resin and polished on a cross section for examination of the accretion internal structure using a Zeiss Axio-Imager M1m digital microscope.

## 2.3 | XRD

Seventy-five of the 77 collected accretions and 6 floor sediment samples were powdered and analysed for bulk mineralogical composition using a Bruker D8 Advance X-ray powder diffractometer with Ni-filtered Cu Kα radiation (1.54 Å) in the Materials Characterisation and Fabrication Platform at the University of Melbourne. Data were collected between 5° and 85° 2θ, with a step size of 0.02° and a scan rate of 1.0 s per step. An incident beam divergence of 0.26° was used with a 2.5° Soller slit in the diffracted beam. The sample was spun at 15 revolutions per minute and the background was fixed manually. Phase identification was completed using Materials Data, Inc., Jade 9.3 and Bruker EVA software with the ICDD PDF-2 and PDF-4 databases, with key mineral phases established for each sample using standard search-matching procedures.

## 2.4 | SEM and EDS

The distribution and morphology of minerals and structures within 6 accretions were established using a Phillips FEI XL30 environmental scanning electron microscope equipped with an OXFORD INCA energy-dispersive X-ray spectrometer at the School of Geography, Earth and Atmospheric Earth Sciences at the University of Melbourne. The instrument has a tungsten filament electron source with a beam of 15 kV and a spot size of 6 μm and was operated in high vacuum mode with a gold coating used to render the samples conductive. The EDS system uses a liquid nitrogen-cooled Si–Li detector with an area of 10 mm$^2$ and an ATW2 thin detector window allowing collection of X-rays between B and U. The elemental composition of each constituent was determined using EDS spot analysis.

## 3 | RESULTS

### 3.1 | Field observations

Accretions, previously termed 'Floor Glazes' (Green et al., 2017a; Green et al., 2017b) in Kimberley rock shelters, have a distinctive appearance: dark-brown to black, smooth and often glossy, expansive coatings that range between thicknesses rarely exceeding 1 cm and mostly ~1–3 mm from the substrate to the accretion surface. The surface homogeneity is largely controlled by the underlying rock morphology and accretions appear thicker within depressions on the depositional surface, with 'flow-like' features observed on some surfaces. In some settings, striations are observed on accretion surfaces or occasionally natural etching has occurred around the edges or in small patches or channels (Figure 2). These accretion surfaces often have a dusty appearance, suggesting that they may no longer be actively developing. Under close inspection, surfaces may show small undulations and may even be botryoidal in texture, often on a microscale, but occasionally visible in the field (Figure 2a [inset]). In cross section, accretions demonstrate highly continuous alternating light and dark layers, occasionally visible to the naked eye in broken fragments (Green et al., 2021).

The accretions mostly occur on low-angle surfaces of up to several square metres, within the shelter dripline, occasionally forming on small ledges, protuberances or in crevices on the shelter walls, where they are often thicker, reflecting the higher potential for accumulation in more sheltered locations (Green et al., 2017a; Watchman et al., 2005) (Figure 3). Very rarely, the accretions have
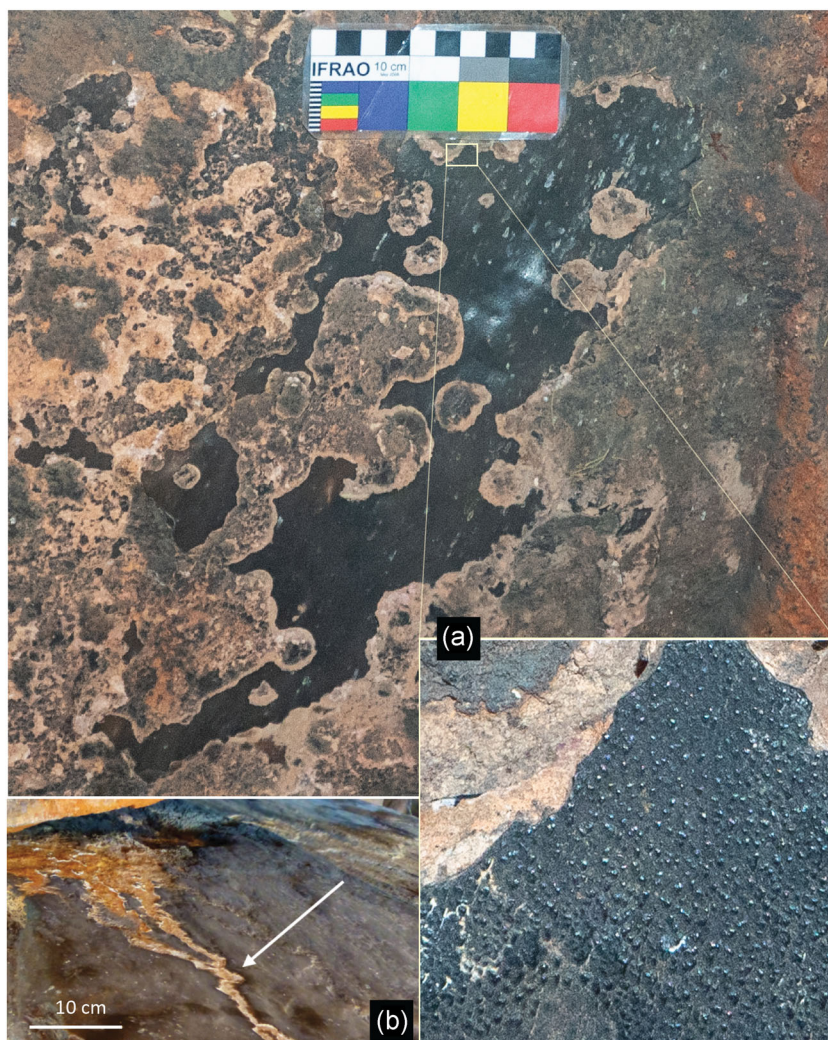


**FIGURE 2** (a) Distinctive erosion pattern occurring on some accretions across the region and demonstrating a microscale botryoidal surface (inset). Sample H634, Barton Plains. (b) Channel etched into an accretion, seemingly related to fluid flow across the surface (white arrow), King George River. See Figure 1 for the location of sampling regions [Color figure can be viewed at wileyonlinelibrary.com]
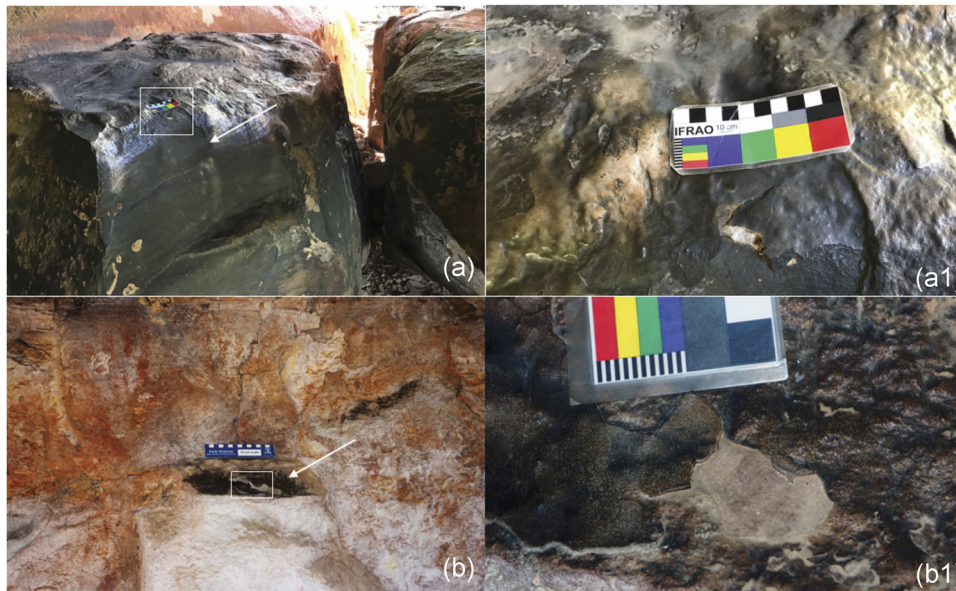
**FIGURE 3** (a) Accretion forming on a boulder at the rock art shelter entrance, within the dripline. Sample H709, Barton Plains. (a1) Zoomed in. (b) Accretion forming on a ledge on the back wall of the rock art shelter. Sample H611, Barton Plains. (b1) Zoomed in. See Figure 1 for the location of sampling regions [Color figure can be viewed at wileyonlinelibrary.com]

been observed on sub-vertical walls in particularly sheltered environments; however, they have never been observed as coating-painted wall panels during fieldwork associated with this study. Field measurements, recorded on 39 accretion surfaces, identify no evidence of preferred orientation in the study area, but 74% of those measured occur at angles of <45°. Accretions observed forming on low-angle, accessible surfaces frequently occur in association with patches of fresh animal urine, often pooling in depressions. However, examples of the accretions occurring in locations inaccessible to local fauna and their vast, uniform extent in some shelters suggest that animal urine cannot be solely responsible for their formation.

The locations in which the accretions are found are generally observed to be damp during the wet season, but sheltered from rain and runoff, with no accretions observed forming in areas that receive direct sunlight, despite being otherwise apparently suitable surfaces within the shelter dripline. Darker accretions occur in damper, shadier areas at the back of shelters, whilst lighter accretions are generally observed in more light-exposed areas.

Examples of engraved accretion surfaces were found to be widespread throughout the north-east Kimberley. These engravings usually consist of multiple, roughly parallel, V-shaped grooves, up to 1 cm wide and ground deep into the accretions (Figure 4a), seemingly utilising the much softer nature of the accretion minerals relative to the hard underlying quartzite. Less frequently, engravings occur as single incisions or shallower scratched motifs, commonly animal tracks (Figure 4b) or simple figures resembling those in painted art on the shelter walls and ceilings. Occasionally, grooves occur alongside cupules that range in size, depth and frequency between sites. Gershtein et al. (2017) describe strikingly similar parallel, linear grooves and cupules engraved into shiny, pale brown mineral accretions covering low-angle shelter surfaces in the rock art region of Lower Pecos, Texas.

In rare instances, accretions were found with an age relationship to painted art. Although the oxalate-rich accretions are very rarely found on the smooth surfaces of sub-vertical wall panels, some limited examples, observed as forming on a ledge or in a crevice on a painted shelter surface, demonstrate a relationship between the accretion and the associated artwork.

## 3.2 | XRD

XRD analysis identified differing proportions of similar minerals in 75 accretions, with all samples containing oxalates, 70 samples containing sulphates and 16 samples containing phosphates (Figure 5a–c). The calcium oxalate dihydrate weddellite occurred in just one sample, with the monohydrate whewellite occurring in all other oxalate-bearing samples. Sulphates include gypsum, anhydrite and bassanite ($2CaSO_4 \cdot H_2O$), with gypsum dominating, occurring in 62 of the 75 samples. Anhydrite was identified in 30 samples and bassanite in 5, possibly as dehydration products of gypsum. Phosphate minerals taranakite ($(K,Na)_3(Al,Fe^{3+})_5(PO_4)_2(HPO_4)_6 \cdot 18H_2O$), brushite ($CaHPO_4 \cdot 2H_2O$), newberyite ($Mg(PO_3OH) \cdot 3(H_2O)$), tinsleyite ($KAl_2(PO_4)_2(OH) \cdot 2H_2O$) and struvite ($NH_4MgPO_4 \cdot 6H_2O$) were identified in 16 samples, comprising more than 50% of two samples. Fifty-six of the 75 samples contained oxalate and sulphate minerals as their sole constituents, with 58 samples containing more than 50% oxalate and 65 samples containing over 30% (when quartz was assumed to be substrate or windblown dust and removed). The average quartz content in the accretion samples was approximately 31%, with the amount present in individual samples varying between 0% and 94%, and the median content across the sample set <20%. This variation is primarily explained by the amount of underlying
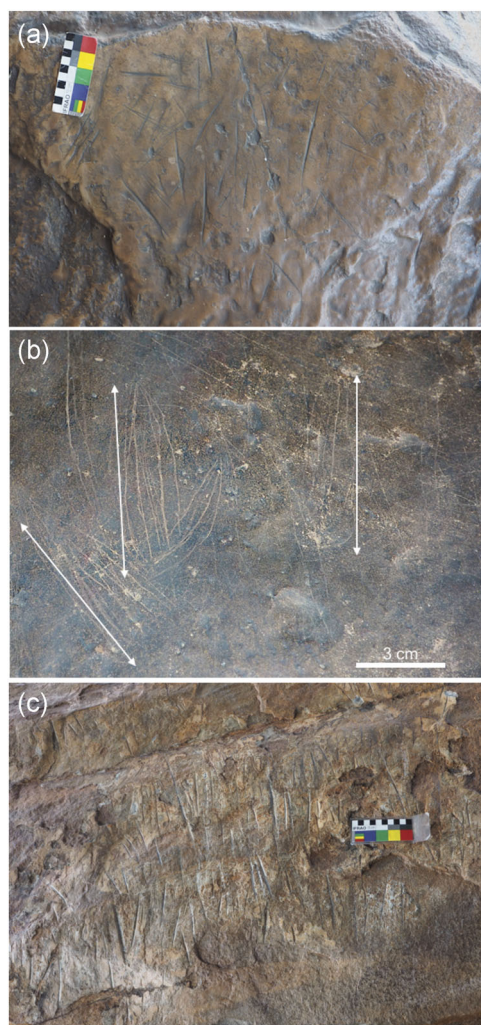
**FIGURE 4** Symbolic/artistic engravings etched into accretions within the Kimberley sampling region. (a) Engraved grooves and small cupules (Sample H415, Drysdale River). (b) Three scratched macropod track marks identified by white arrows (Sample H662, Barton Plains). (c) Engraved grooves, Sample H460, Drysdale River. See Figure 1 for the location of sampling regions [Color figure can be viewed at wileyonlinelibrary.com]

sandstone substrate attached to the analysed sample, with such accretions identified in cross section and containing significantly larger quantities of quartz. Windblown dust may also contribute some minor proportion of quartz to the accretionary layers, with 6 floor sediments from separate shelters composed solely of silicate minerals, containing over 96% quartz, likely sourced from the sandstone bedrock, and some clays.

## 3.3 | SEM and EDS

SEM and EDS analyses of samples identify gypsum as distinctive, elongate platy crystals (Figure 6a,b), returning characteristic EDS spectra peaks at O, S and Ca (Figure 6d). Calcium oxalate crystals are also distinctive, occurring as tetragonal crystals of relatively uniform sizes (Figure 6c) with characteristic EDS spectra peaks at C, Ca and O. Gypsum occurs as individual clusters amongst other accretion components (Figure 6a), intermixed with calcium oxalate crystals and infilling lenticular voids within the accretionary structure (Figure 6b), suggesting that precipitation of some sulphate minerals occurred after deposition of the layer. Evidence of microorganisms in the accretions is also observed, with several unidentified features imaged in samples H076 and J019 (Figure 6e–h), resembling microscale biological structures. In particular, rod-like structures, characteristic of microbes in the *Bacillus* genus (Sitohy et al., 2014) and known to produce oxalate on exposed surfaces in arid conditions (Cheng et al., 2016; Gaylarde et al., 2017; Herve et al., 2016; Martínez et al., 2006; Nuhoglu et al., 2006), are identified in sample J019 (Figure 6h).

## 3.4 | Optical observations

The internal structure of the accretions consists of alternating layers of fine-grained, compact material, with dark layers of varying thicknesses (typically ~30–150 μm) occurring between generally thinner, lighter coloured layers (Figures 7c,d). Small (50–100 μm) lenticular partings occur in regular patterns, often stacked vertically above one another, in both light and dark layers and consistently across the sample set (Figure 7b). It is unclear as to whether these structures, observed in cross section (Figure 7), relate to the small-scale botryoidal texture observed on some accretion surfaces in the field (Figure 2a). These lenticular partings are sometimes infilled with secondary sulphate-rich material apparently precipitating after the layer is deposited (Figures 6b, 7b). All analysed accretions demonstrate sub-micron-scale, black particles dispersed throughout the alternating layers and some display thin, discontinuous layers of coarser-grained red material, occurring between the alternating layers towards the top of the stratigraphy. Although similar, the alternating layers demonstrate differences in grain size, porosity and mineral composition, often appearing to be further divided into micro-laminae under the microscope.

## 4 | DISCUSSION

Dark-brown to black, smooth and often glossy mineral accretions are frequently found in sandstone rock shelters across the Kimberley with their distinctive appearance and softer nature relative to the underlying quartzite, meaning that they commonly host symbolic markings such as engravings and cupules (Figure 4). XRD analyses have identified the accretion mineralogy as dominated by oxalate and sulphate minerals, commonly whewellite and gypsum, with the inconsistent but occasional occurrence of phosphates, suggesting that they are not essential to formation, but may play a facilitating role in some settings (Green et al., 2017a; Green et al., 2017b; Jones et al., 2017; Watchman et al., 2001) (Figure 5). Samples containing phosphates were only found in locations accessible to animals;
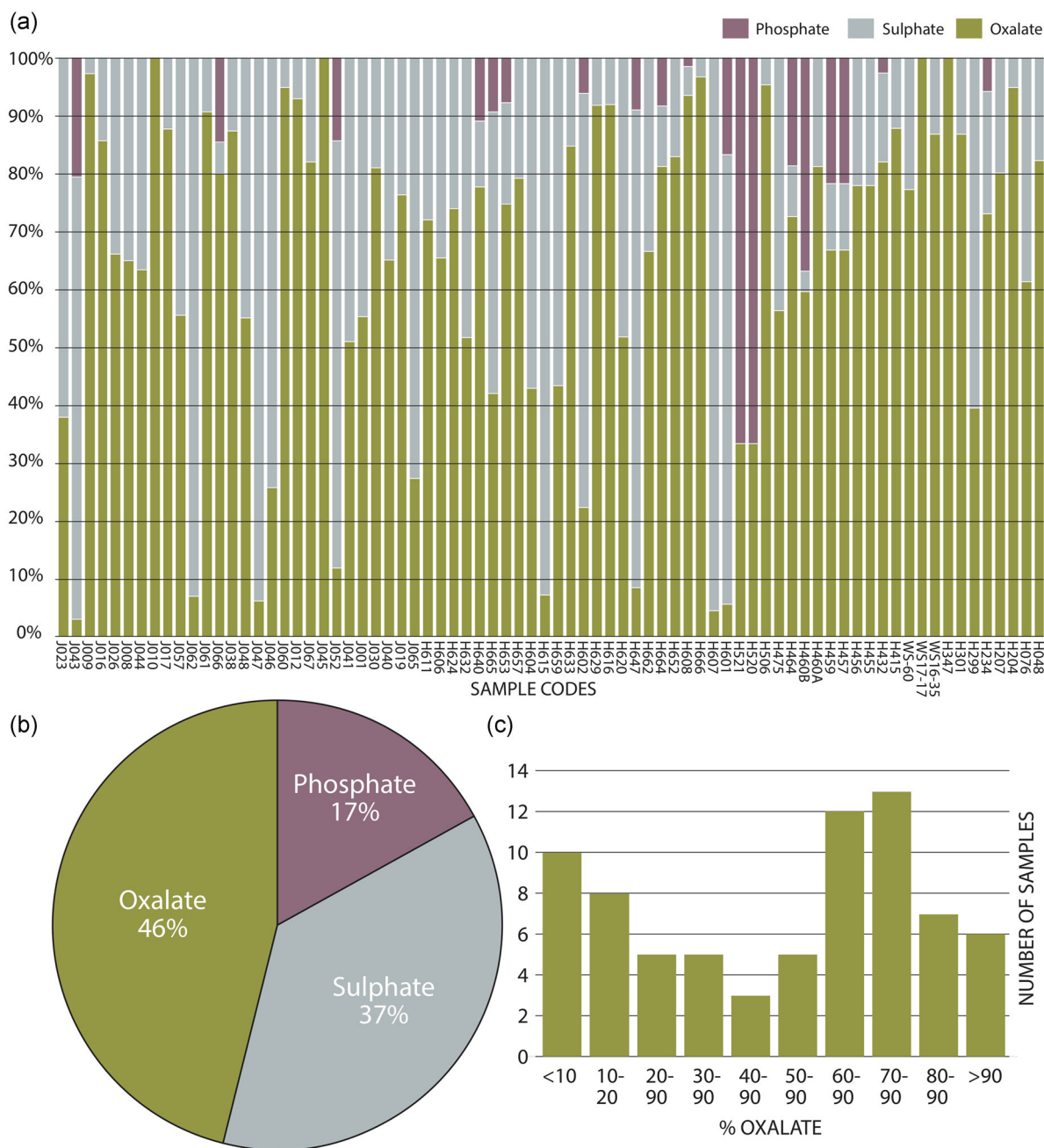
**FIGURE 5** (a) X-ray diffraction data showing the composition of 75 accretions collected across Kimberley between 2015 and 2019. (b) Average composition of the sample set. (c) Histogram showing percentage composition of oxalate across the sample set. Quartz has been removed from the results as cross-sectional analysis revealed this to be the result of bedrock inclusion rather than a component of the accretion structure [Color figure can be viewed at wileyonlinelibrary.com]

however, it is notable that XRD analyses will not detect amorphous material or concentrations of less than ~3% and, consequently, trace levels of phosphates may be present in all samples. The Warton Sandstone, hosting most Kimberley rock shelters (Figure 1), provides no local source for these mineral constituents, necessitating an external origin. The exclusive occurrence of the accretions in shaded areas, crevices and on stable ledges and low-angle surfaces, sheltered from direct wind and rain, indicates their formation is both ultraviolet (UV) light sensitive (Watchman et al., 2005) and restricted to

locations that facilitate the accumulation of calcium- and sulphur-rich material. Windblown particulate matter, sourced from annual bushfires and comprised of both oxalates from the stems, roots and leaves of common plants and lichens (Bodi et al., 2014; and references therein) as well as some carbonate compounds ($CaCO_3$, $MgCO_3$ and $KCO_3$), silicon (Si) and in lower proportions, phosphorous (P), sodium (Na) and sulphur (S) (Bodi et al., 2014; and references therein; Noller et al., 1990; Watchman et al., 2001), provides a likely source for such material.
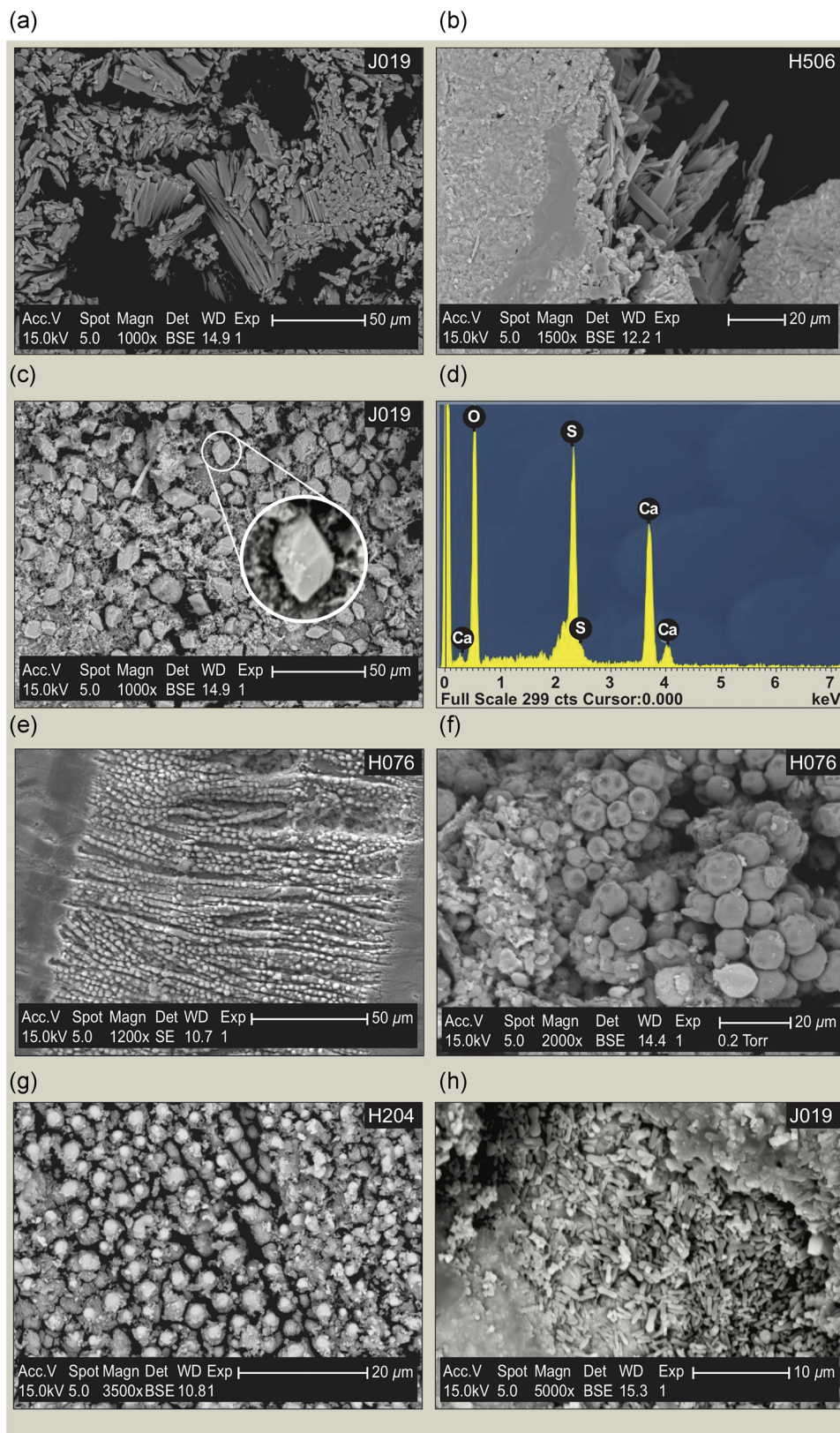
**FIGURE 6** Scanning electron microscopy images of (a) sample J019 and (b) H506 displaying blade-like gypsum crystals, identified as the sole sulphate in X-ray diffraction analysis of these samples, (c) well-defined whewellite crystals also identified in sample J019, (d) energy-dispersive X-ray spectrum analysis of a crystalline lens identified in sample H506 (b), confirming the presence of calcium sulphate. Probable mineralised structures of microbial origin, identified in (e,f) sample H076, (g) sample H204 and (h) sample J019 (resembling the bacterium *Bacillus cereus*), all sampled in the Drysdale River region. See Figure 1 for the location of sampling regions [Color figure can be viewed at wileyonlinelibrary.com]

**FIGURE 7** Cross sections through accretion samples (a) sample J019 viewed under a light microscope, (b) an illustration of the stromatolitic features, identified as small lenticular-shaped, hummocky, layer transgressive structures, occurring in both the light and dark layers and (c) stromatolitic features identified under reflected light in sample (c) H076 (Drysdale River) and (d) H748 (Drysdale River). See Figure 1 for the location of sampling regions [Color figure can be viewed at wileyonlinelibrary.com]
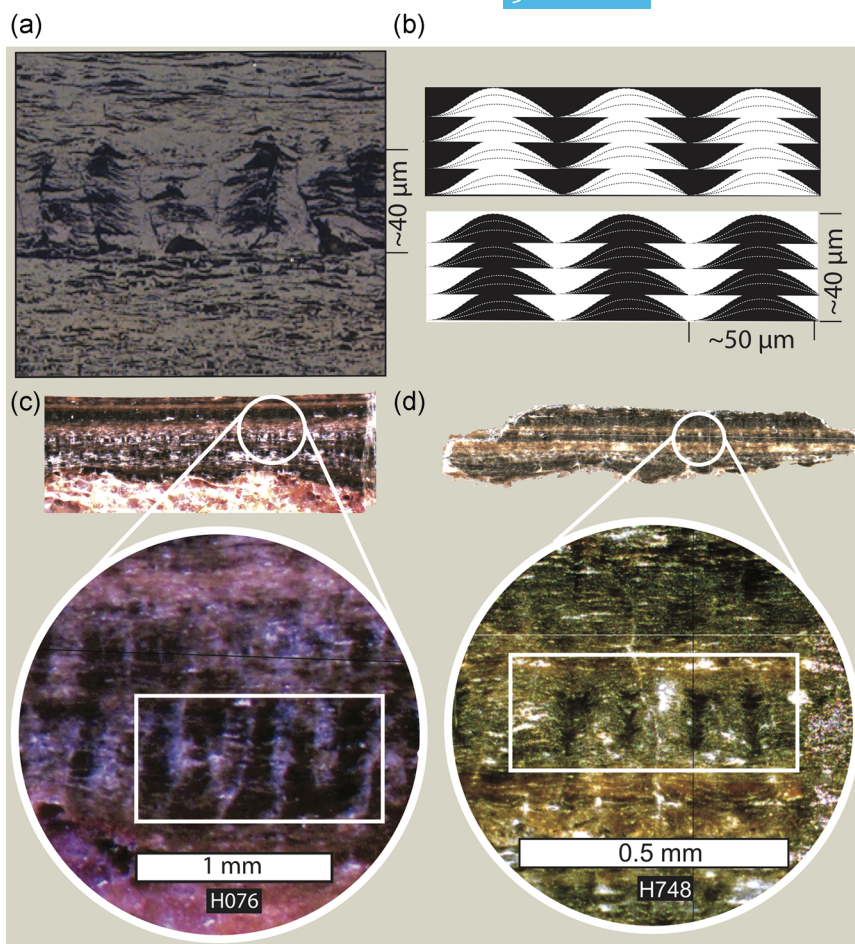
SEM identifies well crystallised, elongate, platy gypsum crystals, often infilling voids within accretion structures and suggesting that at least some sulphate minerals form in situ, crystallising from water (Figure 7a,b) (Watchman et al., 2001). Well-defined calcium oxalate crystals are also identified (Figure 7c), with the dihydrate phase weddellite occurring in just one Kimberley accretion, whilst the monohydrate whewellite occurs in all samples (Figure 5a). In situ precipitation as either the mono- (whewellite) or dihydrate (weddellite) salt occurs when the oxalate anion comes into solution with even low calcium concentrations and the phase is dependent on whether the $Ca^{2+}$ ion or the $C_2O_4^{2-}$ ion in the depositional setting is in excess. Diffusion of $Ca^{2+}$ into an oxalate environment results in whewellite formation, whilst diffusion of $C_2O_4^{2-}$ into a calcium-rich environment forms weddellite (Roberts et al., 2015; and references therein), suggesting that in Kimberley rock shelters, whewellite is formed when calcium-rich material is deposited onto surfaces upon which oxalic acid is already present. Alternatively, the dihydrate may convert into the more stable whewellite during the warmer, drier conditions, prevalent during the Kimberley dry season.

Microscopic analysis of the accretions in cross section reveals internal structures of alternate dark- and light-coloured layers across the sample set, suggesting fluctuating but regularly repeating mechanisms of formation for each. The occurrence of sub-micron-scale, black particles dispersed throughout these alternating layers potentially represents charcoal particles from localised burning, whilst thin, discontinuous layers of coarser-grained red material may be indicative of pigment processing or paint dripping on the accretion surface (David et al., 2019; Watchman, 1993; Watchman et al., 2001). Further research is required to determine whether the origin of this material is aeolian, iron-rich dust or pigment, representing periods of human activity within the rock shelter. Microstructures identified in cross section resemble the accretionary structures in stromatolites (Figure 7) and, alongside unidentified organic inclusions observed in SEM (Figure 6e–h), suggest a comparable formation mechanism involving microbial communities living on Kimberley rock shelter surfaces.

Based on field observations and laboratory analysis, we propose that during the Kimberley dry season, low-angle shelter surfaces facilitate the accumulation of windblown particulate matter sourced from annual bushfires. During the annual wet season, further dissolved mineral constituents are also deposited on these surfaces via aerosol droplets and moisture percolating through sandstone pore spaces (Russ et al., 2000), allowing some sulphate minerals to precipitate in situ (Figure 8a). Wetter conditions facilitate the colonisation of these low-angle shelter surfaces by microbial communities, with the accumulated sulphur-rich material providing a reservoir of moisture and nutrients (Huang et al., 2020). Metabolisation of these nutrients allows colonising microbes to assimilate carbon from the
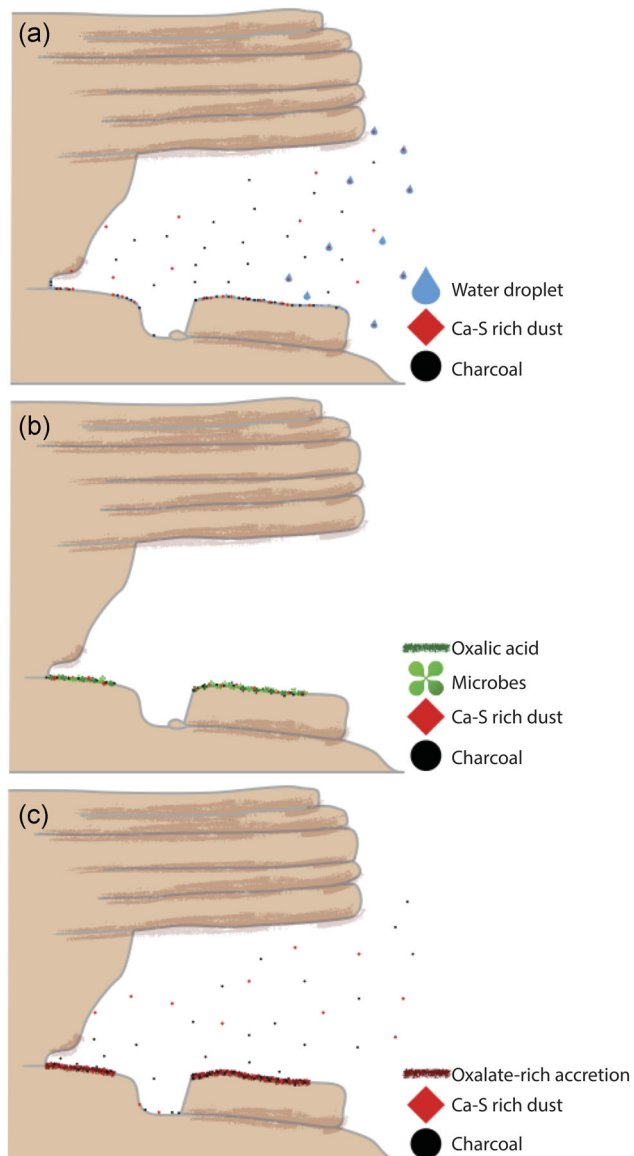
**FIGURE 8** Proposed formation mechanism for oxalate-rich accretions on low-angled surfaces in Kimberley rock shelters. (a) During the Kimberley dry season, low-angle shelter surfaces facilitate the accumulation of calcium- and sulphur-rich, windblown particulate matter sourced from annual bushfires. During the subsequent wet season, further dissolved mineral constituents may also be deposited on these surfaces via aerosol droplets and moisture percolating through sandstone pore spaces allowing some sulphate minerals to precipitate in situ. (b) The moisture and nutrients provided by the accumulated material enable colonisation of these surfaces by microbial communities, and metabolisation of these nutrients results in oxalic acid ($C_2H_2O_4$) formation, which combines with the accumulated aeolian material to form a layer of calcium oxalate. (c) Oxalate precipitation continues until the layer is 'sealed' by the deposition of more windblown particulate matter, most likely the result of a change in environmental conditions, no longer conducive to microbial activity. This cycle repeats, resulting in the laminated, sulphate- and oxalate-rich accretions [Color figure can be viewed at wileyonlinelibrary.com]

atmosphere and excrete this in oxalic acid ($C_2H_2O_4$) (Chalia et al., 2017; Gharieb et al., 1998; Herve et al., 2016; Hess et al., 2008; Jurado et al., 2009; Rusakov et al., 2016; Russ et al., 2000), promoting chelation of cationic constituents (e.g., $Ca^{2+}$) in the accumulated aeolian material and the formation of a layer of calcium oxalate (e.g., whewellite $CaC_2O_4 \cdot H_2O$) (Gorbushina, 2007) (Figure 8b). The rate at which such calcium oxalate deposition occurs is unclear and may vary depending on both the regional and shelter-specific conditions. For instance, many microbes are capable of metabolising the phosphate in minerals such as newberyite ($Mg(PO_3OH) \cdot 3H_2O$) and struvite ($NH_4MgPO_4 \cdot 6H_2O$), commonly found in animal urine (Hernanz et al., 2007), often observed pooling on accretion surfaces. Consequently, in some settings, microbial activity may be facilitated by the presence of animal urine, with the phosphorous content providing an additional nutrient source for microbial activity and phosphate minerals in the accretions potentially fixed to these physically stable surfaces through microbiological processes. Additionally or alternatively, the biochemical release of phosphates following photosynthesis or the degradation of microorganic colonies may be responsible (Watchman, 1985).

Oxalate ions in animal urine may also contribute to accretion formation in such settings; however, our current data do not provide sufficient evidence to distinguish between a urine or microbiological source. Despite a contribution of oxalate ions from separate sources, both would be approximately contemporaneous with the accretion formation, and thus radiocarbon dating of calcium oxalate-rich growth layers would remain reliable.

This process of oxalate precipitation continues until the layer is 'sealed' by the deposition of an overlying, non-oxalate-bearing layer, most likely the result of a change in environmental conditions, no longer conducive to microbial activity (Figure 8c). As this cycle repeats, laminated oxalate and sulphate-rich mineral accretions form expansive oxalate and sulphate-rich coatings, accumulating in layers over long time periods on particular shelter surfaces. As observed, this mechanism would result in accretion distribution spatially dependent on the limit of sunlight penetration into the rock shelter, reflecting the sensitivity of certain microbial communities to UV light (Watchman et al., 2001). Further, microbial secretions used to provide UV light protection as well as to cement accumulated particulate matter and facilitate further adhesion onto the substrate can result in glossy accretion surfaces (Gorbushina, 2007), as observed at many sites in the Kimberley. Consequently dull, dusty accretion surfaces potentially indicate prolonged microbial inactivity.

The much higher occurrence of gypsum in the accretions compared to other sulphate minerals anhydrite and bassanite suggests that whilst gypsum precipitated in situ, anhydrite and bassanite formed only when gypsum became dehydrated. This may be a result of changing shelter moisture regimes, accretion location within a shelter (Watchman et al., 2001) or microbial activity. In the latter, microbes extract moisture from gypsum crystals precipitated in situ (Huang et al., 2020), resulting in phase transformation to dehydrated mineral species such as anhydrite. Consequently, accretions with

higher anhydrite to gypsum ratios may indicate higher microbial activity rates or dehydrated sulphate minerals may represent the initial colonisation of shelter surfaces before oxalate precipitation.

Characteristic weathering patterns observed on many accretion surfaces (Figure 3a) also support a microbiological formation mechanism, potentially representing dissolution of the existing accretion at times or locations where the microbiological habitats became favourable for more extensive and destructive biological activity and consequent chemical weathering by organisms such as lichen, colonising the same surfaces (Chen et al., 2000).

A connection between layered, dark-coloured, oxalate-rich accretions and a microbiological depositional mechanism has been previously discussed by studies in both the Kimberley (Ford et al., 1994; Walsh, 1994; Watchman, 2000; Watchman et al., 2001, 2005) and other parts of the world (Beazley et al., 2002; Roberts et al., 2015; Russ et al., 1996, 1999, 2017; Smith et al., 2009; Whitley et al., 2017). Similar accretions are reported growing on ancient stone monuments and buildings of various historical periods (Bonazza et al., 2014; Del Monte & Sabbioni, 1983; Del Monte et al., 1987; Gaylarde et al., 2017; Rampazzi, 2019; Sabbioni & Zappia, 1991), with their formation linked to microbiological processes involving bacteria, lichens, algae and fungi. Such explanations are largely based on the observation of similarities between the microstructures of oxalate and lichen, the presence of lichen in the shelters and inclusions of cyanobacteria within calcium oxalate layers (Del Monte & Sabbioni, 1983; Del Monte et al., 1987).

In the Kimberley, the link between the limit of oxalate-rich accretion formation and areas exposed to direct rain and sunlight was used to identify microorganisms as the critical formation function (Watchman et al., 2001). However, the microorganisms colonising Kimberley rock shelters have not been identified and may include cyanobacteria (Del Monte & Sabbioni, 1983), micro-stromatolitic algae and fungi (Gadd et al., 2014) or lichens (Russ et al., 1996, 2000, 2017; Smith et al., 2009; and references therein; Watchman, 2000; Watchman et al., 2005), with Gorbushina (2007), suggesting that a collective growth habitat of a combination of organisms is beneficial to the survival of such 'biofilms'. However, the shaded, frequently damp surfaces in which the oxalate-rich accretions are found in Kimberley rock shelters may provide favourable microbiological habitats for some organisms, but not others. Lichens have been identified as a likely source of oxalate crusts in some areas (e.g., Hernanz et al., 2007; Russ et al., 1996, 1999, 2000) as they directly produce crystals of whewellite on their surface. However, lichens require adequate light for photosynthesis and are generally not found in heavily shaded sites. In the Kimberley, while lichens are found on more exposed rock surfaces, they never occur in the environments where oxalate-rich accretions form, at least under present climatic conditions. Blue-green algae or cyanobacteria were identified as the main formation mechanism of oxalate-rich crusts growing on marble surfaces in a Venetian Lagoon in Italy (Del Monte & Sabbioni, 1983). Cyanobacteria are sensitive to UV light, favouring shaded environments; however, they require liquid water rather than water vapour to photosynthesise, and other similar bacteria are only minor producers of oxalic acid (Smith et al., 2009) and thus are unlikely to be responsible for the extensive accretion formation observed in the Kimberley shelters. Microcolonial fungi, common on rock surfaces in arid Australia (Smith et al., 2009), can survive in damp, shaded environments if supplied with an external nutrient source and consequently, we propose that these microorganisms are most likely responsible for the production of calcium oxalate deposits in this setting (Soleilhavoup, 1986; Strobel et al., 2004; Watchman, 1991; Watchman & Jones, 1998; Watchman et al., 2001, 2004).

Importantly, the alternating laminated structure of the accretions indicates discrete intervals of growth and consequently, fluctuation in the conditions of formation, potentially attributed to cyclical changes between wet and dry phases occurring over wide regions and correlated to major palaeoenvironmental regimes (Watchman, 1991; Watchman et al., 2001). In southwestern Texas, oxalate production by epilithic lichens was correlated with dry climate intervals during the middle and late Holocene (Russ et al., 2000); however, accretions in this region are often very thin, limiting the potential to provide detailed insight into the palaeoenvironmental record. Conversely, the detailed internal stratigraphies demonstrated by the Kimberley accretions suggest that they may hold significant potential as palaeoenvironmental archives; however, further work is required to identify the microbial communities responsible for calcium oxalate precipitation, and the conditions under which these thrive, before specific links to palaeoenvironmental conditions can be made.

## 5 | CONCLUSIONS

Relatively thick, oxalate–sulphate mineral accretions in rock shelters across the Kimberley region of north-western Australia preserve a record of mineral deposition in finely laminated, but well crystallised, layers that suggest an extensive history of fluctuating palaeoenvironmental conditions. Extensive field and laboratory observations of the composition and internal structure of these deposits provide strong support for a microbiological formation mechanism. Especially important microscopic evidence is provided by a characteristic internal pattern of vertically stacked, undulating laminations that strongly resemble some kind of micro-stromatolitic growth pattern.

These features, together with the substantial thickness of these accretions compared to similar deposits that have been dated in other parts of the world (Ruiz et al., 2012; Russ et al., 2017; Watchman et al., 2005), suggest slow and undisturbed accumulation over a considerable period of time, making them valuable targets for radiocarbon dating of associated rock art. In sandstone-dominated rock art provinces such as north-west Kimberley, this is particularly valuable as the absence of calcite makes the application of the dominant rock art dating method, uranium-series dating (e.g., Aubert et al., 2014, 2018, 2019; Brumm et al., 2021), much more complex. To date, issues surrounding uranium content, closed system behaviour and detrital thorium contamination have precluded attempts to apply this method to non-calcite-bearing, rock art-associated

accretions. Consequently, the proven reliability of the application of radiocarbon dating to calcium oxalate-rich accretions (Green et al., 2021), often associated with engraved, or in rarer instances, painted art in the Kimberley, has the potential to revolutionise rock art dating by significantly increasing the potential of date-able rock art sites. In addition, sub-sampling of specific oxalate-rich layers may serve as an indicator of environmental conditions favourable for microbial activity during particular periods (Green et al., 2021).

There is a striking association between the occurrence of thick oxalate accretions particularly on low-angle rock shelter surfaces and the common engravings within them. The absence of comparable markings on much harder sandstone surfaces observed in hundreds of rock shelters across the Kimberley region indicates that the engravings have specifically exploited the much softer oxalate–sulphate accretions. Radiocarbon dates of oxalate layers truncated by ground grooves and of later layers infilling them have considerable potential for bracketing the age of these important art works.

## CONFLICT OF INTERESTS

The authors declare that there are no conflict of interests.

## ORCID

*Helen Green* http://orcid.org/0000-0002-7842-6007
*Andrew Gleadow* http://orcid.org/0000-0003-0496-0028
*Damien Finch* http://orcid.org/0000-0002-9447-5685
*Jenna McGovern* http://orcid.org/0000-0002-1876-5170

## REFERENCES

Aubert, M., Brumm, A., Ramli, M., Sutikna, T., Saptomo, E. W., Hakim, B., Morwood, M. J., van den Bergh, G. D., Kinsley, L., & Dosseto, A. (2014). Pleistocene cave art from Sulawesi, Indonesia. *Nature*, *514*(7521), 223–237. https://doi.org/10.1038/nature13422

Aubert, M., Lebe, R., Oktaviana, A. A., Tang, M., Burhan, B., Hamrullah, Jusdi, A., Hakim, A. B., Hakim, B., Zhao, J. X., Geria, I. M., Sulistyarto, P. H., Sardi, R., & Brumm, A. (2019). Earliest hunting scene in prehistoric art. *Nature*, *576*(7787), 442–445. https://doi.org/10.1038/s41586-019-1806-y

Aubert, M., O'Connor, S., McCulloch, M., Mortimer, G., Watchman, A., & Richer-LaFlèche, M. (2007). Uranium series dating rock art East Timor. *Journal of Archaeological Science*, *34*, 991–996.

Aubert, M., Setiawan, P., Oktaviana, A. A., Brumm, A., Sulistyarto, P. H., Saptomo, E. W., Istiawan, B., Ma'rifat, T. A., Wahyuono, V. N., Atmoko, F. T., Zhao, J. X., Huntley, J., Tacon, P. S. C., Howard, D. L., & Brand, H. E. A. (2018). Palaeolithic cave art in Borneo. *Nature*, *564*(7735), 254–257. https://doi.org/10.1038/s41586-018-0679-9

Beazley, M. J., Rickman, R. D., Ingram, D. K., Boutton, T. W., & Russ, J. (2002). Natural abundances of carbon isotopes ($^{14}$C, $^{13}$C) in lichens and calcium oxalate pruina: Implications for archaeological and paleoenvironmental studies. *Radiocarbon*, *44*(3), 675–683.

Bodi, M. B., Martin, D. A., Balfour, V. N., Santin, C., Doerr, S. H., Pereira, P., Cerda, A., & Mataix-Solera, J. (2014). Wild land fire ash: Production, composition and ecohydro-geomorphic effect. *Earth-Science Reviews*, *130*, 103–127. https://doi.org/10.1016/j.earscirev.2013.12.007

Bonazza, A., Natali, C., Ghedini, N., Vaccaro, C., & Sabbioni, C. (2014). Oxalate patinas on stone monuments in the Venetian Lagoon: Characterization and origin. *International Journal of Architectural Heritage*, *9*(5), 542–552.

Brumm, A., Oktaviana, A. A., Burhan, B., Hakim, B., Lebe, R., Zhao, J.-X., Sulistyarto, P., Ririmasse, M., Adhityatama, S., Sumantri, I., & Aubert, M. (2021). Oldest cave art found in Sulawesi. *Science Advances*, *7*(no. 3), eabd4648. https://doi.org/10.1126/sciadv.abd4648

Chalia, S., Baskar, S., Minakshi, P., Baskar, R., & Ranjan, K. (2017). Biomineralization abilities of *Cupriavidus* strain and *Bacillus subtilis* strains *in vitro* isolated from speleothems, Rani cave, Chhattisgarh, India. *Geomicrobiology Journal*, *34*(9), 737–752.

Chen, J., Blume, H.-P., & Beyer, L. (2000). Weathering of rocks induced by lichen colonization—A review. *Catena*, *39*, 121–146.

Cheng, Z. Y., Fernández-Remolar, D. C., Izawa, M. R. M., Applin, D. M., Díaz, M. C., Fernandez-Sampedro, M. T., García-Villadangos, M., Huang, T., Xiao, L., & Parro, V. (2016). Oxalate formation under the hyperarid conditions of the Atacama desert as a mineral marker to provide clues to the source of organic carbon on Mars. *Journal of Geophysical Research: Biogeosciences*, *121*(6), 1593–1604.

Crawford, I. M. (1977). The relationship of Bradshaw and Wandjina art in north-west Kimberley. In P. J. Ucko (Ed.), *Form in indigenous art: Schematisation in the art of aboriginal Australia and prehistoric Europe* (pp. 357–369). Australian Institute of Aboriginal Studies.

David, B., Delannoy, J.-J., Petchey, F., Gunn, R. G., Huntley, J., Veth, P., Genuite, K., Skelly, R. J., Mialanes, J., Harper, S., Ouzman, S., Balanggarra Aboriginal Corporation, Heaney, P., & Wong, V. (2019). Dating painting events through by-products of ochre processing: Borologa, Kimberley, Australia. *Australian Archaeology*, *85*(1), 52–94.

Del Monte, M., & Sabbioni, C. (1983). Weddellite on limestone in the Venice environment. *Environmental Science & Technology*, *17*(9), 518–522. https://doi.org/10.1021/es00115a005

Del Monte, M., Sabbioni, C., & Zappia, G. (1987). The origin of calcium oxalates on historial buildings, monuments and natural outcrops. *Science of the Total Environment*, 67(1), 17–39. https://doi.org/10.1016/0048-9697(87)90063-5

Denniston, R. F., Asmerom, Y., Lachniet, M., Polyak, V. J., Hope, P., An, N., Rodzinyak, K., & Humphreys, W. F. (2013). A Last Glacial Maximum through middle Holocene stalagmite record of coastal Western Australia climate. *Quaternary Science Reviews*, 77, 101–112. https://doi.org/10.1016/j.quascirev.2013.07.002

Donaldson, M. (2012). *Kimberley rock art* (Vol. 1–3). Wildrocks Publications.

Finch, D., Gleadow, A., Hergt, J., Heaney, P., Green, H., Myers, C., Veth, P., Harper, S., Ouzman, S., & Levchenko, V. A. (2021). Ages for Australia's oldest rock paintings. *Nature Human Behaviour*, 5, 310–318. https://doi.org/10.1038/s41562-020-01041-0

Finch, D., Gleadow, A., Hergt, J., Levchenko, V. A., Heaney, P., Veth, P., Harper, S., Ouzman, S., Myers, C., & Green, H. (2020). 12,000-year-old aboriginal rock art from the Kimberley region, Western Australia. *Science Advances*, 6(6), eaay3922. https://doi.org/10.1126/sciadv.aay3922

Ford, B., MacLeod, I., & Haydock, P. (1994). Rock art pigments from Kimberley region of Western Australia: Identification of the minerals and conversion mechanisms. *Studies in Conservation*, 39, 57–69.

Gadd, G., Bahri-Esfahani, J., Li, Q., Rhee, Y., Wei, Z., Fomina, M., & Liang, X. (2014). Oxalate production by fungi: Significance in geomycology, biodeterioration and bioremediation. *Fungal Biology Reviews*, 28(2–3), 36–55.

Gaylarde, C., Ogawa, A., Beech, I., Kowalski, M., & Baptista-Neto, J. (2017). Analysis of dark crusts on the church of Nossa Senhora do Carmo in Rio de Janeiro, Brazil, using chemical, microscope and metabarcoding microbial identification techniques. *International Biodeterioration & Biodegradation*, 117, 60–67.

Gershtein, E. C., Willis, M., Black, S. L., Castaneda, A. M., Buonasera, T., Koenig, C. W., Shipp, J., & Nadel, D. (2017). High-resolution mapping and analysis of shiny grooved rock surfaces: The case study of the Skiles Shelter, Lower Pecos, Texas. *Quaternary International*, 439, 69–82.

Gharieb, M., Sayer, J., & Gadd, G. (1998). Solubilization of natural gypsum ($CaSO_4 \cdot 2H_2O$) and the formation of calcium oxalate by *Aspergillus niger* and *Serpula himantioides*. *Mycological Research*, 102(7), 825–830.

Gorbushina, A. (2007). Life on the rocks. *Environmental Microbiology*, 9(7), 1613–1631.

Green, H., Gleadow, A., & Finch, D. (2017a). Characterisation of mineral deposition systems associated with rock art in the Kimberley region of northwest Australia. *Data in Brief*, 14, 813–835. https://doi.org/10.1016/j.dib.2017.08.029

Green, H., Gleadow, A., Finch, D., Hergt, J., & Ouzman, S. (2017b). Mineral deposition systems at rock art sites, Kimberley, Northern Australia—Field observations. *Journal of Archaeological Science: Reports*, 14, 340–352. https://doi.org/10.1016/j.jasrep.2017.06.009

Green, H., Gleadow, A., Finch, D., Levchencko, V. A., Myers, C., McGovern, J., Heaney, P., & Pickering, R. (2021). Dating correlated microlayers in oxalate accretions from rock art shelters: New archives of paleoenvironments and human activity. *Science Advances*, 7, eabf3632.

Hernanz, A., Gavira-Vallejo, J. M., & Ruiz-Lopez, J. F. (2007). Calcium oxalates and prehistoric paintings. The usefulness of these biomaterials. *Journal of Optoelectronics and Advanced Materials*, 9(3), 512–521.

Herve, V., Junier, T., Bindschedler, S., Verrecchia, E., & Junier, P. (2016). Diversity and ecology of oxalotrophic bacteria. *World Journal of Microbiology and Biotechnology*, 32(2), 28.

Hess, D., Coker, D. J., Loutsch, J. M., & Russ, J. (2008). Production of oxalates in vitro by microbes isolated from rock surfaces with prehistoric paints in the lower Pecos Region, Texas. *Geoarchaeology*, 23(1), 3–11. https://doi.org/10.1002/gea.20208

Hoffmann, D. L., Standish, C. D., García-Diez, M., Pettitt, P. B., Milton, J. A., Zilhão, J., Alcolea-González, J. J., Cantalejo-Duarte, P., Collado, H., de Balbín, R., Lorblanchet, M., Ramos-Muñoz, J., Weniger, G.-C., & Pike, A. W. G. (2018). U-Th dating of carbonate crusts reveals Neandertal origin of Iberian cave art. *Science*, 359(6378), 912–915. https://doi.org/10.1126/science.aap7778

Huang, W., Ertekin, E., Wang, T., Cruz, L., Dailey, M., DiRuggiero, J., & Kisailus, D. (2020). Mechanism of water extraction from gypsum rock by desert colonizing microorganisms. *Proceedings of the National Academy of Sciences of the United States of America*, 117, 10681–10687.

HYSPLIT (HYbrid Single-Particle Lagrangian Integrated Trajectory). (2020). Model access via NOAA ARL READY Website. https://www.ready.noaa.gov/HYSPLIT.php

Jones, T., Levchenko, V. A., King, P. L., Troitzsch, U., Wesley, D., Williams, A. A., & Nayingull, A. (2017). Radiocarbon age constraints for a Pleistocene-Holocene transition rock art style: The northern running figures of the East Alligator River region, western Arnhem Land, Australia. *Journal of Archaeological Science: Reports*, 11, 80–89. https://doi.org/10.1016/j.jasrep.2016.11.016

Jurado, V., Fernandez-Cortes, A., Cuezva, S., Laiz, L., Cañaveras, J. C., Sanchez-Moral, S., & Saiz-Jimenez, C. (2009). The fungal colonisation of rock-art caves: Experimental evidence. *Naturwissenschaften*, 96(9), 1027–1034.

Legge, S., Webb, T., Cooper, T., Lewis, F., Swan, D., Maher, W., & Barton, T. (2016). *EcoFire-Part 1: Kimberley regional fire pattern analysis (2000 to 2014)*. Australian Wildlife Conservancy.

Lewis, D. (1997). Bradshaws: The view from Arnhem land. *Australian Archaeology*, 44, 1–16.

Martínez, I., Escudero, A., Maestre, F. T., de la Cruz, A., Guerrero, C., & Rubio, A. (2006). Small-scale patterns of abundance of mosses and lichens forming biological soil crusts in two semi-arid gypsum environments. *Australian Journal of Botany*, 54(4), 339–348.

McDonald, J., Steelman, K., Veth, P., Mackey, J., Loewen, J., Thurber, C., & Guilderson, T. P. (2014). Results from the first intensive dating program for pigment art in the Australian arid zone: Insights into recent social complexity. *Journal of Archaeological Science*, 46, 195–204. https://doi.org/10.1016/j.jas.2014.03.012

Noller, B. N., Currey, N. A., Ayers, G. P., & Gillett, R. W. (1990). Chemical-composition and acidity of rainfall in the Alligator Rivers region, Northern Territory, Australia. *Science of the Total Environment*, 91, 23–48. https://doi.org/10.1016/0048-9697(90)90286-4

Northern Australian Fire Information (NAFI) Website. (2020). Western Australia-Kimberley. http://www.firenorth.org.au

Nuhoglu, Y., Oguz, E., Uslu, H., Ozbek, A., Ipekoglu, B., Ocak, I., & Hasenekoglu, I. (2006). The accelerating effects of the microorganisms on biodeterioration of stone monuments under air pollution and continental-cold climatic conditions in Erzurum, Turkey. *Science of the Total Environment*, 364(1–3), 272–283.

Pike, A. W. G., Hoffmann, D. L., Garcia-Diez, M., Pettitt, P. B., Alcolea, J., De Balbin, R., Gonzalez-Sainz, C., de las Heras, C., Lasheras, J. A., Montes, R., & Zilhao, J. (2012). U-series dating of paleolithic art in 11 caves in Spain. *Science*, 336(6087), 1409–1413. https://doi.org/10.1126/science.1219957

Quiles, A., Valladas, H., Bocherens, H., Delqué-Količ, E., Kaltnecker, E., van der Plicht, J., Delannoy, J. J., Feruglio, V., Fritz, C., Monney, J., Philippe, M., Tosello, G., Clottes, J., & Geneste, J. M. (2016). A high-precision chronological model for the decorated Upper Paleolithic cave of Chauvet-Pont d'Arc, Ardèche, France. *Proceedings of the National Academy of Sciences of the United States of America*, 113(17), 4670–4675. https://doi.org/10.1073/pnas.1523158113

Rampazzi, L. (2019). Calcium oxalate films on works of art: A review. *Journal of Cultural Heritage*, 40, 195–214.

Roberts, A., Campbell, I., Pring, A., Bell, G., Watchman, A., Popelka-Filcoff, R. S., Lenehan, C. E., Gibson, C. T., & Franklin, N. (2015). A multidisciplinary investigation of a rock coating at Ngaut Ngaut (Devon Downs), South Australia. *Australian Archaeology*, 80, 32–39.

Ross, J., Westaway, K., Travers, M., Morwood, M. J., & Hayward, J. (2016). Into the past: A step towards a robust Kimberley rock art chronology. *PLOS One*, 11(8), 33. https://doi.org/10.1371/journal.pone.0161726

Ruiz, J. F., Hernanz, A., Armitage, R. A., Rowe, M. W., Vinas, R., Gavira-Vallejo, J. M., & Rubio, A. (2012). Calcium oxalate AMS C-14 dating and chronology of post Palaeolithic rock paintings in the Iberian Peninsula. Two dates from Abrigo de los Oculados (Henarejos, Cuenca, Spain). *Journal of Archaeological Science*, 39(8), 2655–2667. https://doi.org/10.1016/j.jas.2012.02.038

Rusakov, A. V., Vlasov, A. D., Zelenskaya, M. S., Frank-Kamenetskaya, O. V., & Vlasov, D. Y. (2016). The crystallization of calcium oxalate hydrates formed by interaction between microorganisms and minerals. In: O. Frank-Kamenetskaya, E. Panova, & D. Vlasov (Eds.), *Biogenic—Abiogenic interactions in natural and anthropogenic systems* (pp. 357–377). Springer. https://doi.org/10.1007/978-3-319-24987-2_28

Russ, J., Hyman, M., Shafer, H. J., & Rowe, M. W. (1990). Radiocarbon dating of prehistoric rock paintings by selective oxidation of organic carbon. *Nature*, 348, 710–711. https://doi.org/10.1038/348710a0

Russ, J., Kaluarachchi, W. D., Drummond, L., & Edwards, H. G. M. (1999). The nature of a whewellite-rich rock crust associated with pictographs in southwestern Texas. *Studies in Conservation*, 44(2), 91–103. https://doi.org/10.2307/1506721

Russ, J., Loyd, D. H., & Boutton, T. W. (2000). A paleoclimate reconstruction for southwestern Texas using oxalate residue from lichen as a paleoclimate proxy. *Quaternary International*, 67, 29–36. https://doi.org/10.1016/s1040-6182(00)00006-9

Russ, J., Palma, R. L., Loyd, D. H., Boutton, T. W., & Coy, M. A. (1996). Origin of the whewellite-rich rock crust in the Lower Pecos region of southwest Texas and its significance to paleoclimate reconstructions. *Quaternary Research*, 46(1), 27–36. https://doi.org/10.1006/qres.1996.0041

Russ, J., Pohl, M. D., Von Nagy, C. L., Steelman, K. L., Hurst, H., Ashby, L., Schmidt, P., Gutierrez, E. F. P., & Rowe, M. W. (2017). Strategies for $^{14}$C dating the Oxtotitlan cave paintings, Guerrero, Mexico. *Advances in Archaeological Practice*, 5(2), 170–183. https://doi.org/10.1017/aap.2016.10

Sabbioni, C., & Zappia, G. (1991). Oxalate patinas on ancient monuments: The biological hypothesis. *Aerobiologia*, 7(1), 31–37.

Sitohy, M. Z., Osman, A. O., & Mahgoub, S. A. (2014). Bioactive proteins against pathogenic and spoilage bacteria. *Functional Foods in Health and Disease*, 4(10), 451–462.

Smith, M. A., Watchman, A., & Ross, J. (2009). Direct dating indicates a mid-Holocene age for archaic rock engravings in arid central Australia. *Geoarchaeology*, 24(2), 191–203. https://doi.org/10.1002/gea.20262

Soleilhavoup, F. (1986). Surfaces of open-air rock art-relationship with biophysical environment and methods of study. *Anthropologie*, 90(4), 743–782.

Strobel, B. W., Kristensen, F., & Hansen, H. C. B. (2004). Oxalate distribution in soils under rhubarb (*Rheum rhaponticum*). *International Journal of Environmental Analytical Chemistry*, 84(12), 909–917. https://doi.org/10.1080/0306731042000268134

Valladas, H., Tisnérat-Laborde, N., Cachier, H., Arnold, M., de Quiros, F. B., Cabrera-Valdes, V., Clottes, J., Courtin, J., Fortea-Perez, J. J., GonzalezSainz, C., & Moure-Romanillo, A. (2001). Radiocarbon AMS dates for Paleolithic cave paintings. *Radiocarbon*, 43(2B), 977–986.

Veth, P., Myers, C., Heaney, P., & Ouzman, S. (2017). Plants before farming: The deep history of plant-use and representation in the rock art of Australia's Kimberley region. *Quaternary International*, 489, 489–45. https://doi.org/10.1016/j.quaint.2016.08.036

Walsh, G. L. (1994). *Bradshaws ancient rock paintings of north-west Australia*. Edition Limitee.

Walsh, G. L. (2000). *Bradshaw art of the Kimberley*. Takarakka Nowan Kas Publications.

Watchman, A. (1985). Mineralogical analysis of silica skins covering rock art. In R. Jones (Ed.), *Archaeological research in Kakadu National Park* (pp. 281–289). Australian National Parks and Wildlife Service.

Watchman, A. (1991). Age and composition of oxalate rich crusts in Northern Territory, Australia. *Studies in Conservation*, 36, 24–32.

Watchman, A. (1993). Evidence of a 25,000-year-old pictograph in northern Australia. *Geoarchaeology*, 8(6), 465–473.

Watchman, A. (2000). A review of the history of dating rock varnishes. *Earth-Science Reviews*, 49(1–4), 261–277. https://doi.org/10.1016/s0012-8252(99)00059-8

Watchman, A., Flood, J., & Chippendale, C. (2004). Dating of rock images in Wardaman country, Northern Territory, Australia. *Rock Art Research*, 21(2), 173–182.

Watchman, A. L., & Jones, R. (1998). Dating rock images in the tropical monsoon region of northern Australia. *Australian Aboriginal Studies*, 1998(2), 64–70. https://search.informit.org/doi/10.3316/ielapa.152233931194370

Watchman, A., O'Connor, S., & Jones, R. (2005). Dating oxalate minerals 20-45 ka. *Journal of Archaeological Science*, 32(3), 369–374. https://doi.org/10.1016/j.jas.2004.10.007

Watchman, A., Ward, I., Jones, R., & O'Connor, S. (2001). Spatial and compositional variations within finely laminated mineral crusts at Carpenter's Gap, an archaeological site in tropical Australia. *Geoarchaeology*, 16(7), 803–824. https://doi.org/10.1002/gea.1021

Welch, D. M. (2015). Aboriginal paintings of Drysdale River National Park, Kimberley. *Western Australia Australian Aboriginal Culture Series*, 10, 322.

Welch, D. M. (1993). Stylistic change in the Kimberley rock art, Australia. In M. Lorblanchet & P. G. Bahn (Eds.), *Rock art studies: The post-stylistic era or where do we go from here? (Oxbow Monograph)* (Vol. 35, pp. 99–113). Oxbow Books.

Whitley, D. S., Santoro, C. M., & Valenzuela, D. (2017). Climate change, rock coatings, and the archaeological record. *Elements*, 13(3), 183–186. https://doi.org/10.2113/gselements.13.3.183